International Journal of Heat and Mass Transfer 221 (2024) 125106

Contents lists available at ScienceDirect

International Journal of Heat and Mass Transfer

journal homepage: www.elsevier.com/locate/ijhmt

Development and assessment of performance of artificial neural networks for prediction of frictional pressure gradients during two-phase flow

A.W. Mauro [a,*], R. Revellin [b], L. Viscito [a]

[a] Department of Industrial Engineering, Università Degli Studi di Napoli Federico II, P.le Tecchio 80, Napoli 80125, Italy
[b] UMR5008, University de Lyon, INSA Lyon, CNRS, CETHIL, Villeurbanne 69621, France

ARTICLE INFO

Keywords:
Two-phase pressure drop
Artificial neural network
Predictive methods
Assessment

ABSTRACT

This paper presents a discussion on several possibilities to predict the frictional pressure gradient during two-phase flow, with both the application of artificial intelligence and the implementation of conventional correlations and predictive methods. To this purpose, a huge database of approximately 8000 data points has been collected from 49 sources available in scientific literature, including 23 working fluids and the following ranges of parameters: mass fluxes from 32.7 to 2000 kg/m^{2}s, saturation temperatures from -190°C to +120°C (reduced pressures from 0.021 to 0.780), tube diameters from 0.5 to 14.0 mm.

This consolidated database has been used to train several artificial neural networks (ANNs), by using only two hidden layers (shallow neural networks) and evaluating the effect of: training and testing datasets choice (either test data included or outside the training domain), the number of neurons for each hidden layer (from 1 to 50), the type of output (either dimensional or non-dimensional), the type and number (from 1 to 22) of input parameters.

The best results (MAPE of 16.8% and 88% of data within ±30%) have been obtained by using the liquid-only two-phase multiplier Φ_{LO}^2 as non-dimensional output and 12 mixed input parameters. Compared to the statistics of well-established literature correlations for frictional pressure drop (best MAPE of 22% and 73% of data points predicted within a ±30% error range, provided by Mauro et al. mechanistic method), the ANN demonstrates therefore a higher general accuracy. However, the use of Artificial Neural Networks does not guarantee a physical trend, which is instead preserved with conventional prediction methods.

1. Introduction

Two-phase flow frequently occurs in a wide range of applications of any kind, from gas/liquid streams in pipes employed in chemical and petroleum industries or natural gas transfer lines, to vapor/liquid flows of refrigerants inside tubes during convective evaporation or condensation in refrigeration and air-conditioning systems. Moreover, two-phase studies are receiving more and more attention in the last years thanks to the increasing demand for efficient and compact systems in several applications, such as avionics, electronics, electrical vehicles and aerospace [1].

The correct prediction of the frictional pressure gradient during two-phase flow is therefore of utmost importance for a correct design of condensers and evaporators, as well as for the estimation of the pumping power required to transport two-phase fluids in all pipelines. On this regard, while pressure losses in a single-phase flow are correctly modeled with well-known correlations, accurate predictions of the frictional pressure gradient in two-phase flow have been proved to be more challenging because of added complexities related to the coexistence of the liquid and the vapor phase and their relative motion and distribution.

Over the last decades, different prediction methods have been proposed by several researchers. They can be mainly classified in two categories, namely homogeneous models and separate flow models, including mechanistic approaches and flow pattern-based correlations. Homogeneous equilibrium models consider the liquid/vapor or liquid/gas mixture as a single-phase flow in which the thermophysical properties are averaged over their corresponding liquid and gaseous values. The resolution of the momentum equation in thermodynamic equilibrium for the estimation of the pressure drop only requires an appropriate definition of the homogeneous viscosity and a correlation for the homogeneous friction factor, which is usually taken from well-known single phase approaches [2,3]. On the other hand, separate flow

* Corresponding author.
E-mail address: wmauro@unina.it (A.W. Mauro).

https://doi.org/10.1016/j.ijheatmasstransfer.2023.125106
Received 6 February 2023; Received in revised form 3 April 2023; Accepted 18 December 2023
Available online 21 December 2023

Nomenclature

Roman

$\frac{dp}{dz}$	frictional pressure gradient [Pa/m]
d	tube diameter [m]
f	friction factor [-]
G	mass flux [kg/m^{2}s]
L	tube length [m]
Pred	reduced pressure [-]
Tsat	saturation temperature [°C]
w	weight or bias [-]
x	vapor quality [-]
X	Martinelli parameter [-]

Greek

Φ^2	two-phase multiplier [-]
α	input value of a neuron
ε	output of a neuron
μ	viscosity [Pa s]
ρ	density [kg/m^3]
σ	surface tension [N/m]

Statistical parameters

δ_{30}	percentage of data points falling into a ±30% error band [%]
MAPE	mean absolute percentage error [%]
MRPE	mean relative percentage error [%]

Subscripts

eq	equivalent
h	hydraulic
L	liquid
LO	liquid only
tp	two-phase
V	vapor
VO	vapor-only

Non-dimensional numbers

La	Laplace number
Fr	Froude number
Pr	Prandtl number
Bd	bond number
We	weber number
Re	Reynolds number

models assume the two phases as flowing with different velocities and are mostly based on the original approach of Lockhart and Martinelli [4], resulting in semi-empirical correlations aimed at the evaluation of two-phase multipliers [5,6,7], two-phase friction factor [8,9], or directly of the two-phase frictional pressure gradient through the combination of the single-phase contributions [10]. Despite this great effort in developing an efficient predictive method, the correlation results are still not completely accurate if tested outside their original database, since significant assumptions of physical phenomena are involved.

For this reason, the Artificial Intelligence (AI) can emerge as a very powerful tool of estimating or predicting data without an explicit understanding of the physical mechanism and are recommended to high non-linear applications and complex engineering problems [11]. Among the available AI techniques, Artificial Neural Networks (ANNs) imitate the neural aspect of the human brain, in which learning is based on experience and repetition rather than the application of principles and equations, and consist of a layered network of neurons, each of them connected to a large number of others [12].

After some pioneering studies [13,14], machine learning methods have been implemented in complex fluid-dynamic systems with different purposes, including the evaluation of the frictional pressure drops. As regards the exclusive use of Artificial Neural Networks, Alizadehdakhel et al. [15] trained an ANN by using only three input parameters (gas and liquid velocities and tube slope to predict the average pressure drop across a 20 mm tube. The authors managed to obtain a mean square error with experimental data of 0.043 Pa/m, even if they found that a better accuracy could be reached by employing commercial CFD codes. Shadloo et al. [16] presented and trained a multiple-layer perceptron neural network for the prediction of the frictional pressure gradient of non-Newtonian liquid/gas mixture, obtaining a minimum Mean Absolute Error (MAE) of 4.58%. Garcia et al. [17] applied artificial neural networks for the prediction of pressure drop during evaporation of refrigerant R407C in horizontal tubes having diameters of 4.5 mm and 8.0 mm. The authors considered diameter, mass flux, vapor quality and saturation pressure as model input parameters, whereas the ANN structure (number of neurons and number of hidden layers) was determined based on the results accuracy. The proposed ANN, trained with 127 data points, was able to detect the experimental pressure gradient with a Mean Absolute Error (MAE) of 6.11%. Regarding the choice of the input parameters, some researchers autonomously identified the most influencing factors based on the real physics of the phenomenon, as managed by Longo et al. [18] for pressure drop data in a plate heat exchanger. The same approach was followed by Barroso-Maldonado et al. [19], by using a physics-based rationale to determine dimensional and non-dimensional parameters as inputs of their ANN-based correlation for frictional pressure gradient of non-azeotropic mixtures. Machine learning tools and pipelines were instead implemented by Najafi et al. [20] and by Ardam et al. [21] to identify the most promising set of input parameter to obtain frictional pressure drop of air-water data and R134a data, respectively. A parametric importance analysis, including the Group of Method Data Handling (GMDH), was also chosen by Lopez-Belchi et al. [22] and by Khosravi et al. [23] to estimate the correct set of parameters to feed their machine learning system trained to estimate the pressure gradient of several refrigerants. Swarm plots and Kendall coefficient analysis were performed by Qiu et al. [24] to graphically provide a sensitivity evaluation on possible input parameters. The authors used a consolidated database of 2787 experimental frictional pressure gradient data in mini and micro-channels and critically developed four different machine learning based regression models. They found that their ANN model, conceived with 23 non-dimensional input parameters, could predict the experimental values with an error lower than 10%, whereas other machine learning approaches (KNN regressions, Extreme Gradient Boosting, XGBoost, and Light Gradient Boosting Machine, Light-GBM) were tougher to be implemented with worse outcomes. Similar outcomes were found by Khosravi et al. [23] and by Nie et al. [25], who found that ANN models for two-phase frictional pressure drop led to a better accuracy when respectively compared with Support Vector Regression (SVR) models and with XGBoost approaches.

In this context, the main objective of this work is to evaluate to what extent the Artificial Neural Networks can be employed in successfully predicting the two-phase frictional pressure gradient, with respect to the accuracy of deterministic models. Different neural networks are then developed and a critical analysis is carried-out, testing their accuracy and sensibility by changing the ANN structure and the number and type of the input parameters. The assessment of some benchmark correlations and of the developed ANNs is also proposed by using a large database in a wide range of operating conditions in terms of mass flux, reduced pressure, tube diameter and vapor quality.

2. Basic concepts of Artificial Neural Networks (ANNs)

An Artificial Neural Network (ANN) is a mathematical tool inspired by the biological human nervous system. The main characteristics of an ANN are: learning adaptation, robustness, massive parallelism, abstraction and generalization, and they try to extract linear combinations of one or more input variables, mapping the dependent variable as non-linear functions of derived features from the input values. Practically, as shown in Fig. 1a, they consist of a layer of input variables, several (one or more) layers of hidden neurons and one layer of one or multiple outputs. Each layer is made up of a series of neurons, that are fully connected to the preceding layer (from which the input is received) and to the subsequent layer (from which they influence). Fig. 1b shows the configuration of a generic k neuron belonging to any of the intermediate layers. The interconnection with all neurons in the neighboring cluster is represented by a variable called weight (w), and M is the number of neurons located in the previous layer. A bias factor w_{bias} is also used to treat the incoming information. With linear accumulation, each neuron combines information from weights and bias to produce the initial output ε:

$$\varepsilon_k = \sum_{m=1}^{M} \tau_m w_{m,k} + w_{bias} \tag{1}$$

The output ε is then used to feed an activation function, that basically executes a nonlinear transformation and determines the output of the neuron itself.

The critical aspect of an ANN is the training step that defines the learning process, consisting in having new experience with the modification of the strength of the connections among neurons. This procedure is generally called algorithm, in which the input values are given to the network together with the desired output. The purpose of the training algorithm is to minimize the global error level, with weights and biases randomly chosen to be progressively adjusted so that the network attempts to obtain the desired output. When a satisfactory level of performance is reached (with respect to statistical parameters such as Mean Squared Error MSE or Mean Absolute Percentage Error MAPE), the training phase stops, and the network uses the final set of weights as a predictive tool. According to the ANN architecture, there are different training methods that can perform the learning process according to the individual objectives, such as the accuracy of the results, computational time and complexity of the algorithm itself. For predicting purposes, the most popular technique to perform the learning process is the Error Back-Propagation [26]. This tool relies on two steps (forward and backward passes) recursively performed until the satisfactory performance is reached. In the forward pass, the ANN output is calculated according to the sets of input and of weights imposed, therefore computing an error with respect to the effective target. This error is then used to calculate the weight values of the output layer. In the subsequent backward step, the error is propagated towards the input layer computing the adjustment of the synaptic weights of the hidden layers.

This Error Back-Propagation algorithm requires continuous and differentiable activation functions. For their choice, linear functions are generally used in the output layer, whereas the hyperbolic tangent or the sigmoid are the most common transfer functions for the hidden layers, since their derivative simplify the implementation of the algorithm.

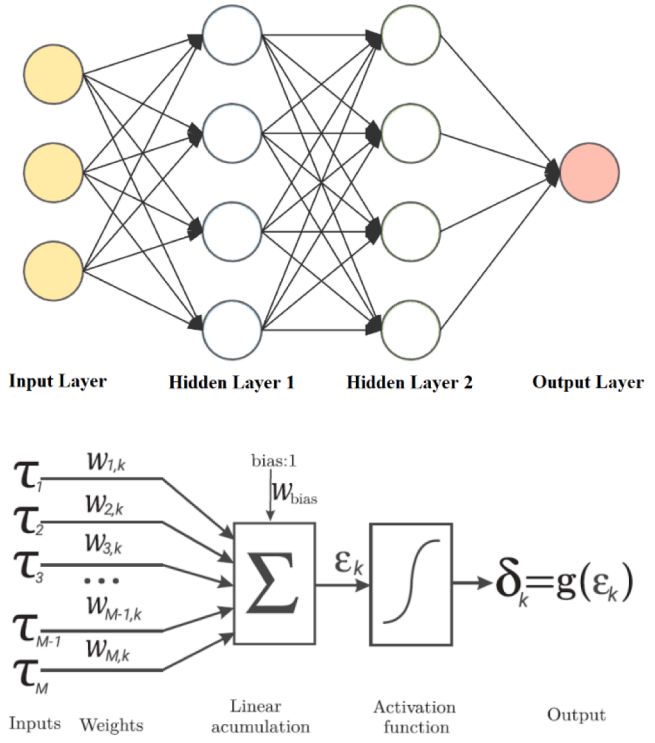

Fig. 1. (a) Structure of a generic ANN having 2 hidden layers, with multiple input values and a single output; (b) General configuration of a neuron [19].

3. Database description

The development of an artificial neural network requires a huge amount of data for its correct learning process. For this reason, more than 8000 experimental local frictional pressure gradient values have been collected from several studies in literature, including vertical and horizontal tubes, and covering a wide range of fluids and operating conditions in terms of mass flux, reduced pressure and tube diameter. The vapor quality range (0-1) is also completely covered in any source. The description of the database, including all the ranges related to each parameter of interest, along with the working fluids are shown in Table 1. Particularly, 47 sources from literature have been reviewed to collect 8003 pressure gradient values, since 2000 and up to the present days, covering 23 refrigerants and cryogenic fluids (methane, nitrogen), mass fluxes from 32.7 to 2000 kg/m^{2}s, saturation temperatures from -190 to +120°C (reduced pressures from 0.021 to 0.780), pipe lengths from 70 to 6000 mm. The collected frictional pressure drop data values, used as model output, widen from 0.008 to 1322 kPa/m. All data refer to smooth circular tube and pure substances or mixtures (all points related to the presence of lubricant or taken in enhanced surfaces such as microtubes have been discarded and do not belong to the present database). Both vertical (2%) and horizontal (98%) configurations are included in the dataset, even if in the first case the pressure gain/loss related to the liquid head is subtracted from the total measured pressure drop values. Also, in case of non-negligible vapor quality variation along the tested tube, (if not explicitly done by the original authors) the momentum contribution was calculated by using the void fraction model of Rouhani and Axelsson [27] and subtracted from the whole pressure gradient, in order to obtain only the effective frictional contribution.

In order to consider only reliable data for the subsequent assessment operations, the entire database has been filtered to eliminate points whose goodness was unsure. Since the uncertainty value for each experimental point was not available to this purpose, the Müller-Steinhagen and Heck [10] correlation was implemented, with all points having a relative error greater than 100% or lower than -100% excluded from the analysis. This specific predictive method as filter *a-priori* was chosen because it was developed using a very large database (more than 9000 points) and thanks to its worldwide proven recognized accuracy in a wide range of operating conditions. After this operation, the number of remaining points is 7912.

The qualification of the database is shown in Fig. 2, in terms of reduced pressure, tube internal diameter, mass flux, vapor quality, vapor-to-liquid density ratio and vapor-to-liquid viscosity ratio. Most of the points (more than 70%) have reduced pressures lower than 0.5 and mass velocities lower than 500 kg/m^{2}s, reflecting the real application

Table 1
Summary of the main parameters in the paper for the collected database.

Authors	Fluid(s)	G [kg/m^{2}s]	T_{sat} [°C]	d [mm]	L [mm]	N of points
Wu et al. [28]	R744	200; 400	15	1.7	1000	20
Wetzel et al. [29]	R744	300	[-21; -10]	14	256	37
Pehlivanoglu et al. [30]	R744	100; 400	[-30; -15]	6.1	150	36
Mastrullo et al. [31]	R744	201; 349	[-7.8; 5]	6	1200	111
Wu et al. [32]	R744	300; 600	[-40; 0]	1.42	300	273
Park and Hrnjak [33]	R744	200; 400	[-30; -15]	6.1	150	24
Cho and Kim [34]	R744	318	0; 5	4; 7.72	5000	12
Pettersen [35]	R744	190; 380	0; 20	0.81	500	20
Pettersen [36]	R744	190; 570	0; 10	0.81	500	31
Grauso et al. [37]	R744, R410A	152; 513	[-9; 42]	6	1000	1089
Ono et al. [38]	R744	100; 380	10	3.76	1000	28
Kim and Hrnjak [39]	R744	100; 200	-15	11.2	1000	11
Katsuta et al. [40]	R744	400	0; 10	3	500	34
Del Col et al. [41]	R290	200; 800	40	0.96	220	46
Lillo et al. [42]	R290	149; 300	25; 35	6	237.5	140
Charnay et al. [43]	R245fa	300; 1000	60; 120	3	350	149
Sempertegui-Tapia and Ribatski [44]	R134a, R11234ze (E), R1234yf, R600a	200; 1400	31; 41	0.98	180	404
Padilla et al. [45]	R1234yf, R134a, R410A	300; 760	10; 20	10.85	1000	811
Del Col et al. [46]	R134a, R1234yf	200; 800	30; 50	0.96; 1.23	440	132
Longo et al. [47]	R143a, R290, R1270	150; 800	30; 40	4	1000	170
Longo et al. [48]	R32	200; 800	30; 40	4	1000	85
Song et al. [49]	R14	200; 650	[-54; -85]	4	200	104
Diehl et al. [50]	R290, R600a	240; 480	25	1	366	121
Pabon et al. [51]	R1234yf	200; 400	20; 30	3.2; 8	1000	83
Lillo et al. [52]	R32	150; 500	25; 40	6	237.5	127
Grauso et al. [53]	R134a, R1234ze (E)	149; 514	[-2.7; 12.1]	6	1000	704
Ducoulombier et al. [54]	R744	200; 1400	[-10; 5]	0.529	191	591
Fazelnia et al. [55]	R1234yf	95; 410	30	8.2	700	196
Quiben and Thome [56]	R410A, R22, R134a	150; 600	5	8; 13	2035	288
Zhuang et al. [57]	R170	101; 256	[-32; 2]	4	200	244
Zhuang et al. [58]	Methane	100; 254	[-108; -91]	4	200	133
Cavallini et al. [59]	R134a, R125, R32, R410A, R236ea	100; 750	30; 50	8	1600	142
Chen et al. [60]	Nitrogen	235; 560	[-188; -183]	1.98; 2.92	600	90
Zhang and Webb [61]	R134a, R22, R404A	400; 1000	25; 65	3.25	914	56
Longo et al. [62]	R134a, R152a, R1234yf, R1234ze (E)	75; 600	30; 40	4	1000	351
Qi et al. [63]	Nitrogen	33; 262	-170	1; 2	300	58
Revellin and Thome [64]	R134a, R245fa	350; 2000	26; 35	0.509; 0.79	70	244
Arcasi et al. [65]	R1233zd	150; 500	25; 65	6	237	95
Lima et al. [66]	R717	55; 160	[-14.7; 13]	14	403	54
Qiu et al. [67]	R600a	150; 300	20	8	2400	36
Bashar et al. [68]	R134a, R1234yf	100; 200	30	2.14	852	34
Aprea et al. [69]	R407C, R417A	350; 500	2; 26	6	6000	51
Xu et al. [70]	R1234yf, R134a, R410A	540; 870	21; 31	1.8	200	182
Yang et al. [71]	R1234yf, R134a	200; 1200	14	4	600	68
Zakaria et al. [72]	R1234yf	80; 320	31	8.3	670	27
Chen et al. [73]	Nitrogen	140; 300	[-190; -185]	2.92; 3.96	1000	46
Maqbool et al. [74]	R717	100; 500	23; 43	1.2; 1.7	245	215

utility. The vapor quality range is instead well distributed from the onset of boiling up to the complete evaporation of the liquid phase. A significant amount of data (almost 2500 points) is taken for typical commercial diameters used in the refrigeration sector (6.0 mm), even if a non-negligible number of data is caught for minichannel geometries (lower than 2.0 mm).

4. ANN development and assessment

4.1. Imposed settings and conditions

A critical aspect is the definition of the artificial neural network architecture (number of layers, number and types of inputs, the activation function of each layer and the training algorithm). For the present analysis, the ANN has been developed with MATLAB software and the embedded *fitnet* function is employed with the following settings: the maximum number of epochs (training iterations) has been fixed to 2000; only 2 hidden layers have been created, since shallow neural networks are particularly suitable for regression problems [1]. There is no specific procedure to evaluate the optimum number of hidden neurons, and it must be identified case by case. For this work, an equal number of neurons is considered for both hidden layers, and the chosen amount is the result of a sensitivity analysis. The performance indicator (to be minimized during the training process) is the Mean Absolute Percentage Error (MAPE), defined as follows, where n is the number of points used for comparison:

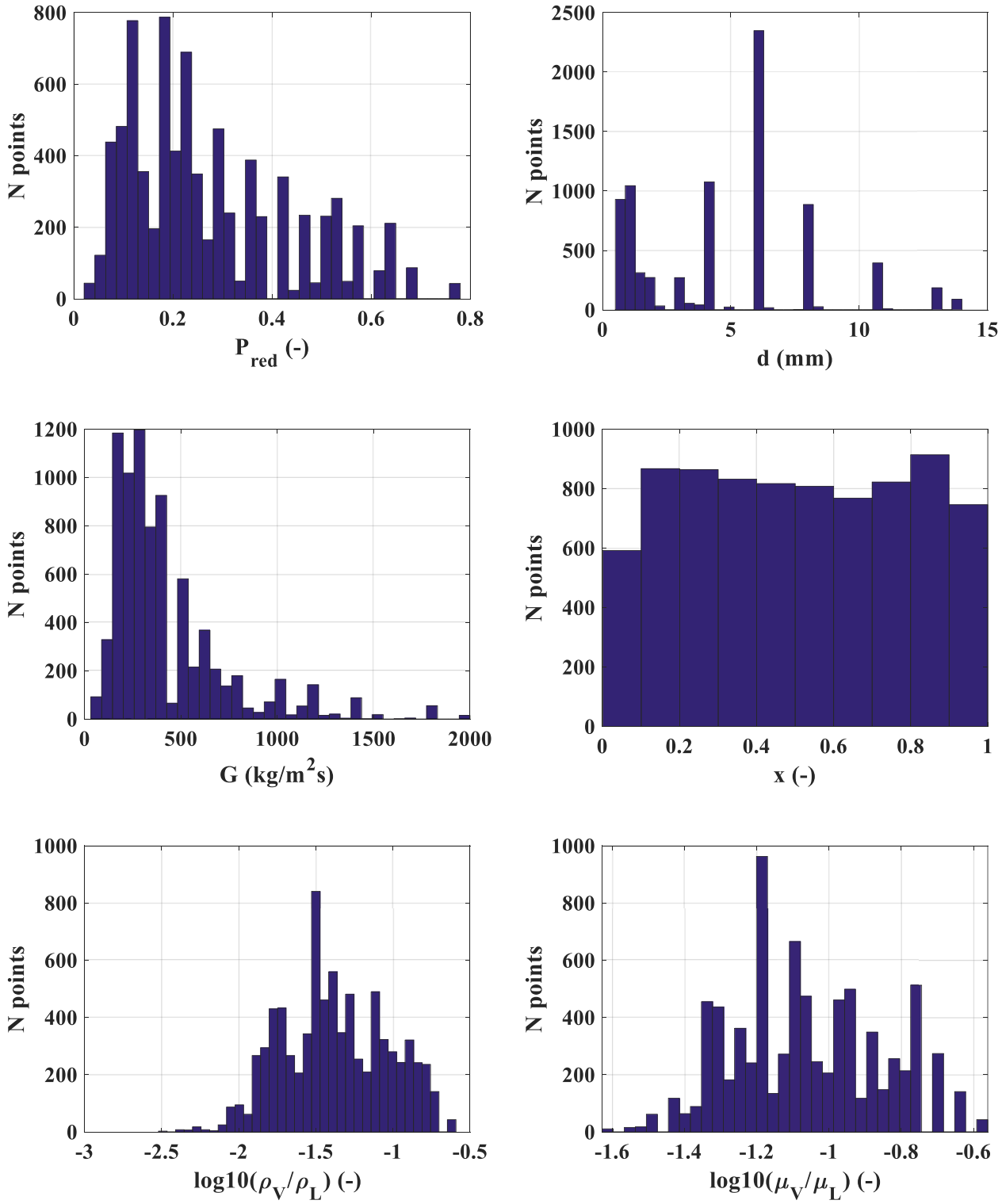

Fig. 2. Qualification of the filtered database used for the assessment. Distribution of: (a) reduced pressure; (b) tube internal diameter; (c) mass flux; (d) vapor quality; (e) vapor-to-liquid density ratio; (f) vapor-to-liquid viscosity ratio.

$$MAPE = \frac{1}{n}\sum_{i=1}^{n}\frac{\left|\frac{dp}{dz_{pred}} - \frac{dp}{dz_{real}}\right|}{\frac{dp}{dz_{real}}}\cdot 100 \tag{2}$$

For the subsequent statistical analysis, the percentage of data points falling into an error range of ±30% and the Mean Relative Percentage Error, MRPE, have also been used. Particularly, the definition of the MRPE is given as follows:

$$MRPE = \frac{1}{n}\sum_{i=1}^{n}\frac{\left(\frac{dp}{dz_{pred}} - \frac{dp}{dz_{real}}\right)}{\frac{dp}{dz_{real}}}\cdot 100 \tag{3}$$

The optimization algorithm is the Levenberg-Marquardt back-propagation one, which is particularly suitable for training small- and medium-sized problems. The following conditions have instead been

changed for the sensitivity analysis:

- Database separation, according to 2 scenarios, graphically shown in Fig. 3. Rationale 1: 60% of the points used for training, and 40% used for validation and testing. The split process is random inside the domain. Rationale 2: 60% of the points used for the training process, belonging to the inner area of the domain (reduced pressures included between 0.06 and 0.75, tube diameters from 1.5 to 10 mm and mass velocities included in the range 150-1600 kg/m^{2}s). In the first case, the interpolation ability of the ANN is tested, whereas for rationale 2 an extrapolation is instead required.
- Type (either dimensional or non-dimensional) and number of inputs (from 1 to 22) and types of output (among dimensional $\frac{dp}{dz_{fr}}$ and non-dimensional parameters).
- In order to establish the best possible structure, for each setting and rationale the network has been trained starting from 1 neuron in both hidden layers, increasing this number up to 50. The best configuration was chosen as the one providing the lowest Mean Absolute Percentage Error (MAPE) when implemented for the independent test database.

4.2. Effect of the number of neurons and of the database rationale, with dimensional input/output

The effect of the number of neurons for the two database splitting scenarios is described in this section. For such analysis, the frictional pressure gradient $\frac{dp}{dz_{fr}}$ has been chosen as dimensional output, by also fixing the dimensional inputs as the minimal set of 8 parameters involved in the phenomenon, according to any mechanistic method: mass flux G, tube diameter d, vapor quality, density (liquid and vapor ρ_L, ρ_V), viscosity (liquid and vapor μ_L, μ_V) and surface tension σ. Fig. 4 shows the calculated MAPE versus the number of neurons composing the two hidden layers, for database splitting rationale 1 (Fig. 4a) and database splitting rationale 2 (Fig. 4b). The blue line refers to the MAPE index evaluated for the training database and the green line to the MAPE index calculated for the testing independent database. As regards rationale 1 (randomly 60%/40%, Fig. 4a), the mean error has not a particular trend with the number of neurons, and it remains quite stable except for some spikes. Moreover, there is not a large difference between the training and the testing database, thus encouraging the use of an artificial neural network within the extreme values of the training domain. For rationale 2 (Fig. 4b), instead, the mean errors related to the testing database are significantly higher than those calculated with the training set. This implies that the use of an ANN outside the extreme values of the training domain can bring to very large errors and therefore extrapolation procedures are not recommended. One point worth noting is that the MAPE index related to the independent database averagely increases with the number of neurons, thus highlighting also an overfitting issue in case of rationale 2.

In each case, the ANN that minimizes the MAPE index is highlighted in red in Fig. 4. This analysis on the number of neurons is always performed for any configuration and rationale chosen. All the following results shown in Table 2 will be referred to the sole best ANN structure, intended as the number of neurons of the hidden layers minimizing the MAPE index when used with the independent testing database.

4.3. Effect of the number and type of input and output

The analysis and the statistic evaluation of the developed artificial neural networks has been carried out for different types and number of inputs (dimensional, non-dimensional, mixed) and of output (dimensional dp/dz_{fr}, and non-dimensional parameters). The assessment of the ANN is carried out by calculating the Mean Absolute Percentage Error (MAPE), Mean Absolute Relative Error (MRPE), and the number of data points falling within an error range of ±30% (δ_{30}). Table 2 summarizes the main characteristics of the implemented ANNs, indicating also their best structure after the node sensitivity analysis (number of neurons in the 2 hidden layers). All the statistical parameters refer to the independent testing database. The computational time required for the training phase has also been indicated (referring to our machine, namely a i9-12900K 3.19 GHz core and 64GB of RAM memory), showing that in all cases it remains within reasonable values. The time required to run any ANN was found instead negligible (less than 10 seconds for all the database).

By using the dimensional output $(dp/dz)_{fr}$ and the minimum number of 8 independent variables that influence the phenomenon, the best MAPE obtainable with the chosen options is quite high (82.7%), even if the 62.2% of the points is predicted within a ±30% error range. A graphical evaluation of the calculated error for this ANN as a function of the effective experimental frictional pressure gradient is shown in Fig. 5a, highlighting that the greatest predicting issues refer to the lowest experimental values. As shown in the previous section, by using the internal database for training and the external domain for testing (rationale 2, see Fig. 3b), the statistic considerably worsens, with a lower MAPE, but a significant amount of data out of the fair predictable zone (δ_{30}=17.2%).

The use of a non-dimensional output was seen to increase the accuracy of the neural networks. To obtain a non-dimensional pressure drop, different options can be pursued, such as the two-phase multiplier Φ^2, either based on the liquid (Φ^2_L, where the reference is the effective liquid mass flow rate flowing alone across the entire diameter of the tube) or the liquid-only (Φ^2_{LO}, in which the reference is the total mass flow rate, considered liquid, flowing alone across the entire diameter of the tube) pressure drop.

$$\Phi^2_{\mathrm{L}} = \frac{(dp/dz)_{fr}}{(dp/dz)_L} \tag{4}$$

$$\Phi^2_{\mathrm{LO}} = \frac{(dp/dz)_{fr}}{(dp/dz)_{LO}} \tag{5}$$

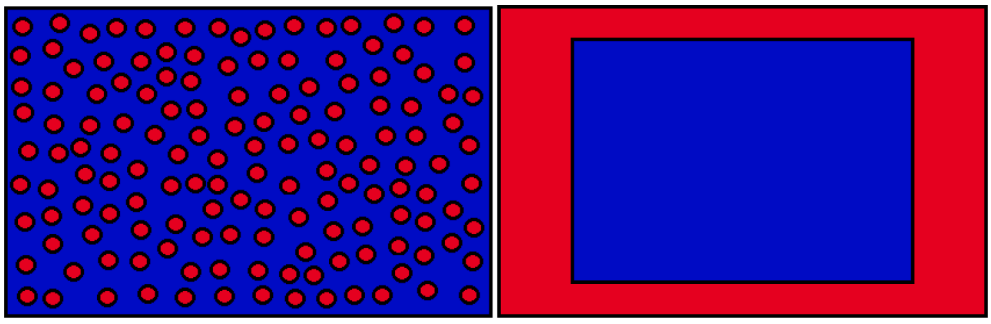

Fig. 3. Possible database splitting for training and testing phases. (a) Rationale 1: 60% for training (blue zone), randomly distributed in the entire domain. (b) Rationale 2: 60% for training (blue zone), excluding the extreme points of the domain (in terms of tube diameter, reduced pressure and mass flux).

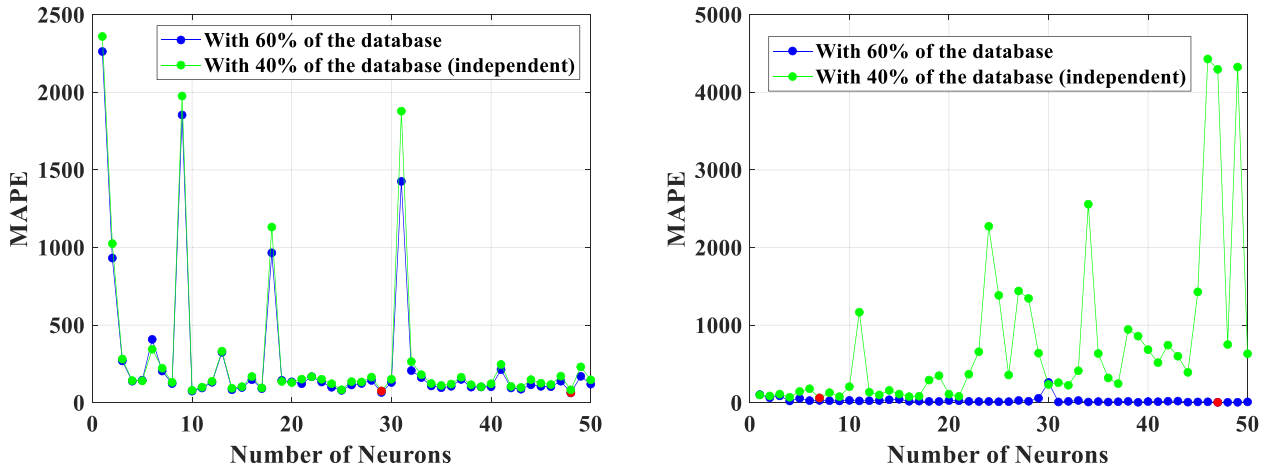

Fig. 4. MAPE calculated for the training and the testing databases as a function of the number of neurons, by considering the frictional pressure gradient as output and G, d, x, ρ_L, ρ_V, μ_L, μ_V, σ as model input parameters. The network configuration minimizing the MAPE index for both databases is highlighted in red. (a) Database splitting rationale 1 (randomly 60%/40%); (b) Database splitting rationale 2 (60% training with points in the inner domain and 40% testing points outside).

Table 2
Summary of the developed ANNs with their main features in terms of output, inputs, database splitting criterion, number of neurons minimizing the MAPE index for the testing independent database, and statistical indexes. All ANNs are made up of 2 hidden layers.

#ANN	Output	Database splitting (rationale 1 or 2)	Input(s)	Best ANN (number of neurons)	Computational time required for training [min]	MAPE [%]	MRPE [%]	δ_{30} [%]
1	$\frac{dp}{dz_{fr}}$	1	$G, d, x, \rho_L, \rho_V, \mu_L, \mu_V, \sigma$	29	3.4	82.7	15.1	62.2
2	$\frac{dp}{dz_{fr}}$	2	$G, d, x, \rho_L, \rho_V, \mu_L, \mu_V, \sigma$	7	0.8	63.5	-32.2	17.2
3	Φ_L^2	1	$G, d, x, \rho_L, \rho_V, \mu_L, \mu_V, \sigma$	38	3.6	32.5	-12.5	62.3
4	Φ_L^2	1	X^2	8	0.3	45.4	-14.3	42.9
5	Φ_L^2	1	$\frac{1-x}{x}, \frac{\rho_V}{\rho_L}, \frac{\mu_V}{\mu_L}$	9	0.5	43.3	12.6	44.4
6	Φ_L^2	1	$\frac{1-x}{x}, \frac{\rho_V}{\rho_L}, \frac{\mu_V}{\mu_L}, We_V$	8	0.4	43.0	11.4	43.6
7	Φ_L^2	1	$\frac{1-x}{x}, \frac{\rho_V}{\rho_L}, \frac{\mu_V}{\mu_L}, We_V, Fr_V$	39	3.2	44.2	11.1	50.9
8	Φ_L^2	1	$\frac{1-x}{x}, \frac{\rho_V}{\rho_L}, \frac{\mu_V}{\mu_L}, We_V, Fr_V, Re_L, Re_V, Re_{LO}$	8	1.1	40.3	3.8	48.4
9	Φ_L^2	1	$Bd, Fr_{tp}, Fr_L, Fr_{LO}, Fr_V, Fr_{VO}, La_L, La_V, P_{red}Pr_L, Pr_V, Re_{eq}, Re_L, Re_{LO}, Re_V, Re_{VO}, We_{tp}, We_L, We_{LO}, We_V, We_{VO}, X$	18	2.4	33.9	-6.4	64.1
10	Φ_L^2	1	$G, d, x, \rho_L, \rho_V, \mu_L, \mu_V, \sigma, \frac{1-x}{x}, \frac{\rho_V}{\rho_L}, \frac{\mu_V}{\mu_L}, (\rho_L - \rho_V)$	8	1.0	32.6	-2.4	67.5
11	Φ_{LO}^2	1	$G, d, x, \rho_L, \rho_V, \mu_L, \mu_V, \sigma, \frac{1-x}{x}, \frac{\rho_V}{\rho_L}, \frac{\mu_V}{\mu_L}, (\rho_L - \rho_V)$	32	2.9	16.8	-0.5	87.6
12	Φ_{LO}^2	2	$G, d, x, \rho_L, \rho_V, \mu_L, \mu_V, \sigma, \frac{1-x}{x}, \frac{\rho_V}{\rho_L}, \frac{\mu_V}{\mu_L}, (\rho_L - \rho_V)$	3	0.6	29.5	-5.1	61.3

By employing the liquid two-phase multiplier, the accuracy of the artificial neural network substantially increases when used in interpolating mode (rationale 1): with only one input (Martinelli parameter X, in ANN #4 of Table 2) and 8 neurons in the hidden layers, the MAPE index is 45.4%, with almost 62.3% of the points predicted within ±30%. By increasing the number and type of non-dimensional inputs, from ANN #4 to #9, with the last having 22 dimensionless numbers, and some of them even not directly involved in the phenomenon (such as Laplace number, Prandtl number,…), the accuracy improves only slightly, having a MAPE of 33.9% and δ_{30}=64%. The type of input seems to have a greater effect than the amount of parameters involved: with the minimum number of 8 dimensional and physics-based inputs (ANN #3 of Table 2), the MAPE is around 32%, and therefore as good as the most complicated and time-consuming non-dimensional input case #9. Slightly better results are obtained with mixing dimensional and non-dimensional inputs, including only physics-based parameters: ANN #10, with 12 mixed inputs and 12 neurons in the hidden layers, provides a similar MAPE as ANN #3 of 32.6%, but increases to 67.5% the number of points predicted in the ±30% error range.

Finally, by employing the liquid-only two-phase multiplier, Φ_{LO}^2 and the same set of mixed parameters, the statistics in rationale 1 (ANN #11) is considerably improved (MAPE=16.8% and δ_{30}=87.6%), with a reduced number of points reaching very high relative errors, as shown in Fig. 5b, probably due to the best fitting ability of the liquid-only two-phase multiplier, that is experimentally represented by lower values than those of the liquid two-phase multiplier. Moreover, the Φ_{LO}^2 output

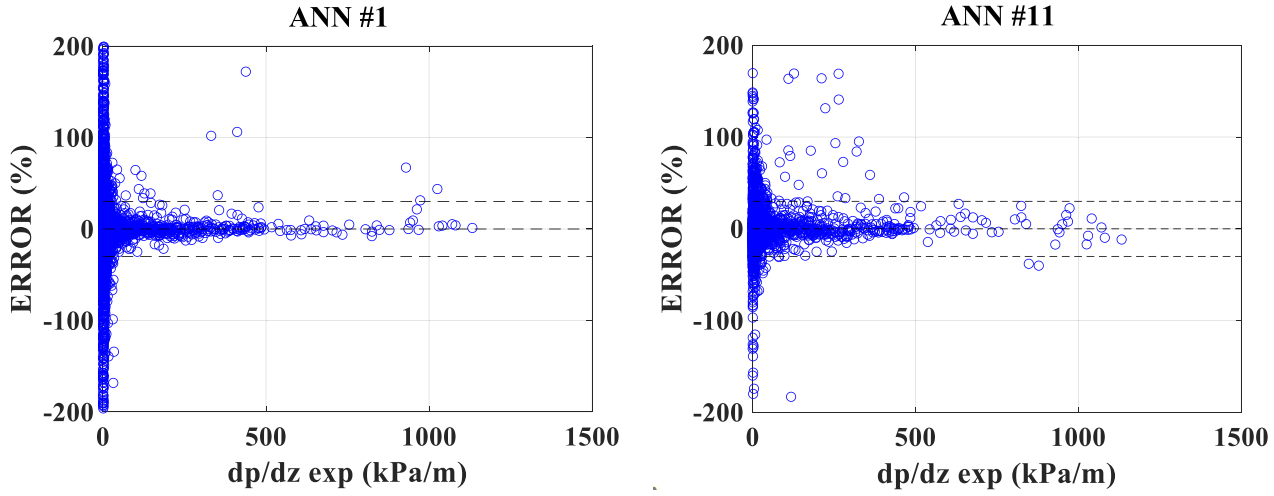

Fig. 5. Error in prediction of the developed ANNs as a function of the experimental frictional pressure gradient. (a) ANN #1 in Table 2 (dimensional output and 8 dimensional inputs); (b) ANN #11 in Table 2 (non-dimensional Φ^2_{LO} output and 12 mixed inputs).

parameter better manages to predict the frictional pressure drop out of the training database: the calculated MAPE for rationale 2 (ANN #12 in Table 2) is 29.5% and δ_{30}=61.3%.

5. Assessment of conventional predictive methods and comparison

For comparison purposes, different conventional prediction methods have been implemented and tested with the present database. Among the numerous tool available in scientific literature, some of the most quoted ones (a homogeneous flow model, a two-phase liquid multiplier-based model, a two-phase liquid-only multiplier based model, the Müller-Steinhagen and Heck correlation and a mechanistic method) are here briefly presented and tested with the database at disposal.

The homogenous model is based on the assumption that no slip occurs between the liquid and the vapor phase, and therefore the two-phase flow is treated as a homogeneous mixture of liquid and vapor having averaged properties. According to the homogeneous model, the frictional pressure drop for a steady-state flow is:

$$\left(\frac{dp}{dz}\right)_{fr} = \frac{2f_{tp}G^2}{d_h\rho_{tp}} \tag{6}$$

where d_h is the hydraulic diameter; the two-phase density ρ_{tp} is obtained as:

$$\rho_{tp} = \left(\frac{x}{\rho_V} + \frac{1-x}{\rho_L}\right)^{-1} \tag{7}$$

For the evaluation of the two-phase Fanning friction factor f_{tp}, the typical hyperbolic expression for laminar flow and the Blasius equation for turbulent flow can be used:

$$f_{tp} = 16/Re_{tp} \text{ for } Re_{tp} < 2300 \tag{8}$$

$$f_{tp} = 0.079 \cdot Re_{tp}^{-0.25} \text{ for } Re_{tp} > 2300 \tag{9}$$

Several homogeneous models are then available for the evaluation of the two-phase viscosity, needed for the calculation of the two-phase Reynolds number. In this work, the simple interpolation method of Cicchitti [75] has been employed, together with the modification of the homogeneous model by Tibiriçá et al. [74]:

$$\mu_{tp} = x \cdot \mu_V + (1-x) \cdot \mu_L \tag{10}$$

Different models assuming a non-negligible velocity slip between the two phases are generally called separated flow models. On this regard, the methods by Lockhart and Martinelli [4], Friedel [7], Moradkhani et al. [75] and Kim and Mudawar [75] have been tested in this work. The first attempts the calculation of the liquid two-phase multiplier according to the Martinelli parameter X:

$$\Phi_L^2 = 1 + \frac{C}{X} + \frac{1}{X^2} \tag{11}$$

where C is a constant whose value depends on the characteristics of the single liquid and vapor phases (whether laminar or turbulent).

The Friedel correlation [7], instead, aims at the evaluation of the liquid-only two-phase multiplier Φ^2_{LO} by taking into account the effects of inertia, buoyancy and surface tension with the definition of the Froude and Weber non-dimensional numbers:

$$\Phi^2_{LO} = C_1 + \frac{3.24 C_2 C_3}{Fr^{0.045} We^{0.035}} \tag{12}$$

The C_1, C_2 and C_3 parameters are a function of the vapor quality, density and viscosity of the liquid and vapor phases.

The Müller-Steinhagen and Heck [10] correlation proposes instead a sort of geometrical average over the liquid-only and vapor-only single-phase frictional pressure gradients. Despite its simplicity, it is worldwide recognized as one of the most effective predictive methods for the evaluation of the frictional pressure gradient during two-phase flow within a considerable range of substances and pipe dimensions.

$$\frac{dp}{dz_{fr}} = \left\{\frac{dp}{dz_{LO}} + 2\left[\frac{dp}{dz_{VO}} - \frac{dp}{dz_{LO}}\right]x\right\} \cdot (1-x)^{0.33} + \frac{dp}{dz_{VO}} \cdot x^3 \tag{13}$$

Finally, the mechanistic models aim to a better understanding of the occurring phenomenon by using mass and momentum balances applied over a specific elementary control volume. Among them, the recent Mauro et al. [76] prediction method is tested for the present database. The resolution algorithm and the complete set of expressions, including the closure equations needed for the entrainment ratio, the atomization rate, the shear stress at the wall and at the liquid-vapor interface, are available in the original reference [76] and are not reported here for conciseness purposes. Since this method was developed for annular flow regime, all data points have been classified according to the flow pattern maps of Cheng et al. [77] in case of CO_2 as working fluid and of Wojtan et al. [78] otherwise. Only annular flow data have therefore been considered to test Mauro et al. [76] mechanistic model.

All the statistical parameters are summarized in Table 3, whereas a graphical comparison for the best methods in shown in Fig. 6, in which the red lines refer to an error band of ±30%. Müller-Steinhagen and

Table 3
Assessment of the two-phase pressure drop conventional prediction methods.

Correlation	MAPE (%)	MRPE (%)	$\delta_{\pm 30\%}$ (%)
Homogeneous (Cicchitti et al. [75])	27.8	-18.3	60.2
Tibiriçá et al. [74]	24.2	+5.7	71.4
Lockhart and Martinelli [4]	96.1	+86.4	31.1
Friedel [7]	29.2	+9.3	68.1
Moradkhani et al. [75]	48.1	-6.7	33.3
Kim and Mudawar [76]	27.9	-0.9	63.2
Müller-Steinhagen and Heck [10]	22.4	-8.7	73.0
Mauro et al. [76]	27.7	-8.1	73.1

Heck correlation [10] provides the best statistics (although its use as outliers filter has conditioned this analysis), followed by the model of Tibiriçá et al. [74] and the mechanistic method of Mauro et al. [76] for annular flow, that provides the largest discrepancies for low pressure gradients, likely to be characterized by a higher relative uncertainty and/or probably not originally belonging to annular flow regime. The homogeneous model of Cicchitti [75] also works surprisingly well for the entire database, whereas the correlation of Lockhart and Martinelli [4] for the liquid two-phase multiplier gives high errors and a low percentage of data points falling in a ±30% error range.

5.1. Trends with vapor quality and comparison with ANNs

Some of the developed ANNs and the chosen correlations have been finally tested against an independent dataset not used for the training process (R1234ze fluid, mass flux of 200 kg/m^{2}s, saturation temperature of -2.6°C and tube diameter of 6.0 mm, by Grauso et al. [53]), by providing the predicted frictional pressure gradient trend versus vapor quality, as shown in Fig. 7. Almost any conventional predictive model (except for that of Lockhart and Martinelli) is able to catch the experimental increasing and decreasing trend, with some numerical discrepancies whose magnitude depends on the specific method used. As summarized also in Table 3, the correlations of Müller-Steinhagen and Heck [10] and Friedel [7], and the Mauro et al. [76] mechanistic model better cover the experimental values, especially for vapor qualities up to 0.65. On the contrary, by choosing the best working developed ANNs, the physical trend with vapor quality is not preserved, except for the Φ^2_{LO} output neural network #11, that fairly covers the experimental values. The remaining tools with Φ^2_L as non- dimensional output provide a good accuracy for low vapor qualities but then the prediction is underestimated by a large amount. A non-physical trend is also observed for the best neural network developed with the dimensional output $(dp/dz)_{fr}$.

6. Conclusions

Both artificial intelligence-based methods (shallow neural networks) and conventional correlations have been implemented in this paper to evaluate their accuracy in predicting the two-phase frictional pressure gradient in smooth tubes. To this purpose, more than 8000 two-phase frictional pressure drop experimental points have been collected and filtered from 49 independent sources in scientific literature. Several artificial shallow neural networks (having two hidden layers with an

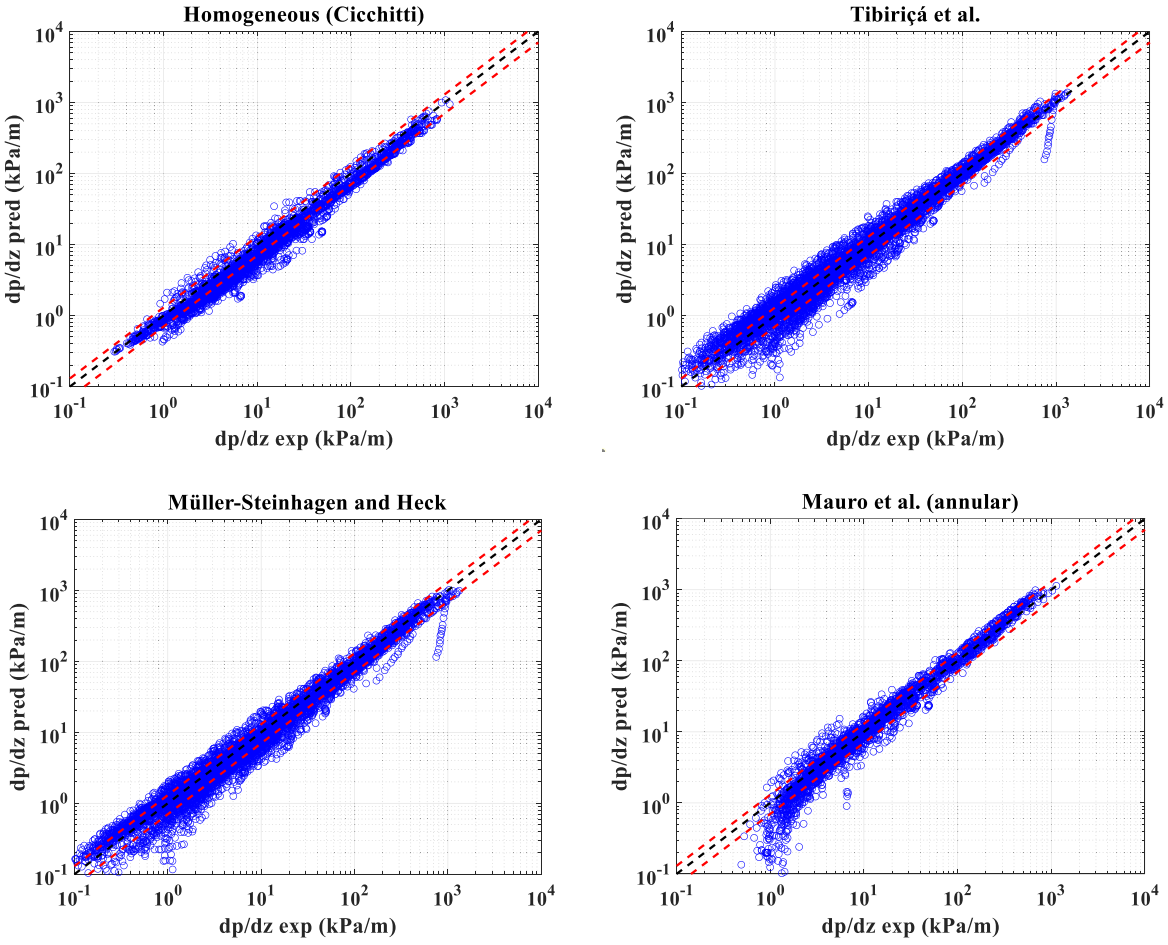

Fig. 6. Experimental versus predicted frictional pressure gradient for the best working conventional predictive methods. (a) Homogeneous model (Cicchitti); (b) Tibiriçá et al.; (c) Müller-Steinhagen and Heck; (e) Mauro et al.

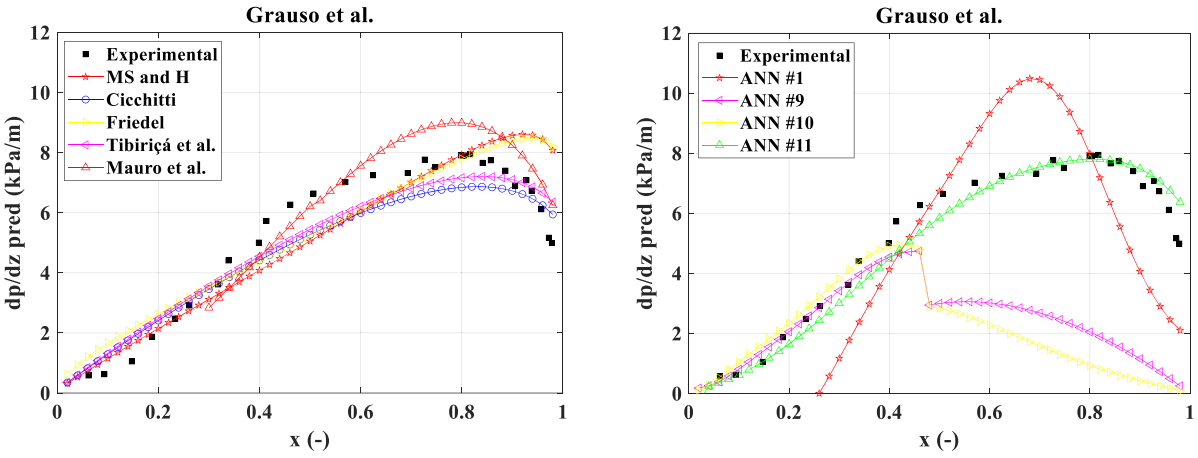

Fig. 7. Experimental and predicted frictional pressure gradient trends with vapor quality. All data refer to the following conditions: R1234ze fluid, mass flux of 200 kg/m^{2}s, saturation temperature of -2.6°C and tube diameter of 6.0 mm. (a) Assessment of some conventional correlations and (b) of some developed ANNs.

equal number of neurons each) as predictive tools have therefore been developed by changing some key settings such as number and type of inputs, type of output and the database shares for training and testing processes. The main outcomes of this research are summarized as follows:

- The ANN can be fairly used as interpolation tool (in which the testing dataset is included in the training domain), since the MAPE index is similar when calculated for both datasets.
- By using the ANN as extrapolating tool (in which the testing dataset is outside the domain of the training set of data) is not recommended, since the MAPE index is very different when calculated for the training and the testing database.
- There is not a significant difference in accuracy when increasing the number of neurons in the hidden layers from 1 to 50. In this work, the best ANN configuration is always chosen as the one that minimizes the MAPE index when used with the independent testing database.
- When using the liquid two-phase multiplier Φ_L^2 as non-dimensional output of the neural network, the accuracy improves only slightly by increasing the number of input non-dimensional parameters (from 1 to 22, including non-physical ones).
- The use of the liquid-only two-phase multiplier Φ_{LO}^2 as non-dimensional output for the neural network and the use of mixed input parameters (both dimensional and non-dimensional) provides the best accuracy, with a MAPE of 16.8% and almost 88% of the testing points within a ±30% error range.
- Most of the conventional predictive methods have a fair accuracy, with a calculated MAPE index between 22% (Müller-Steinhagen and Heck correlation [10]) and 29% (Friedel correlation [7]), and between 60% (homogeneous model with Cicchitti [75] two-phase viscosity) and 73% (Mauro et al. [76] mechanistic model) of data points falling in an error range of ±30%.
- Most of the developed ANNs (except for the one with Φ_{LO}^2 as non-dimensional output) do not provide realistic trends with vapor quality, whereas this physical aspect is preserved with almost all the conventional predictive methods.

CRediT authorship contribution statement

A.W. Mauro: Conceptualization, Data curation, Methodology, Resources, Supervision, Writing – review & editing. **R. Revellin:** Conceptualization, Data curation, Supervision. **L. Viscito:** Data curation, Formal analysis, Investigation, Methodology, Writing – original draft, Writing – review & editing.

Declaration of Competing Interest

The authors declare that they have no known competing financial interests or personal relationships that could have appeared to influence the work reported in this paper.

Data availability

Data will be made available on request.

References

[1] S.M. Kim, I. Mudawar, Universal approach to predicting two-phase frictional pressure drop for mini/micro-channel saturated flow boiling, Int. J. Heat Mass Transf. 58 (2013) 718–734.
[2] D.R.H. Beattie, P.B. Whalley, Simple two-phase frictional pressure drop calculation method, Int. J. Multiph. Flow 8 (1982) 83–87.
[3] M.M. Awad, Y.S. Muzychka, Effective property models for homogeneous two-phase-flows, Exp. Therm. Fluid Sci. 33 (2008) 106–113.
[4] R.W. Lockhart, R.C. Martinelli, Proposed correlation of data for isothermal two-phase, two-component flow in pipes, Chem. Eng. Prog. 45 (1949) 39–48.
[5] L. Sun, K. Mishima, Evaluation analysis of prediction methods for two-phase flow pressure drop in mini-channels, Int. J. Multiph. Flow 35 (2009) 47–54.
[6] K. Mishima, T. Hibiki, Some characteristics of air-water two-phase flow in small diameter vertical tubes, Int. J. Multiph. Flow 22 (1996) 703–712.
[7] L. Friedel, Improved friction pressure drop correlation for horizontal and vertical two-phase pipe flow, European Two-Phase Flow Group Meeting (1979), Paper E2, Ispra, Italy.
[8] A. Cioncolini, J.R. Thome, Pressure drop prediction in annular two-phase flow in macroscale tubes and channels, Int. J. Multiph. Flow 89 (2017) 321–330.
[9] C. Lombardi, C.G. Carsana, A dimensionless pressure drop correlation for two-phase, two-component flow in pipes, Chem. Eng. Prog. 45 (1949) 39–48.
[10] H. Müller-Steinhagen, K. Heck, A simple friction pressure drop correlation for two-phase flow in pipes, Chem. Eng. Prog. 20 (1986) 297–308.
[11] T. Cong, G. Su, S. Qiu, W. Tian, Applications of ANNs in flow and heat transfer problems in nuclear engineering: a review work, Prog. Nucl. Energy 62 (2013) 54–71.
[12] D.J. Livingstone, Artificial Neural Networks, Humana Totowa Publisher, 2009, https://doi.org/10.1007/978-1-60327-101-1.
[13] J. Thibault, B.P.A. Grandjean, A neural network methodology for heat transfer data analysis, Int. J. Heat Mass Transf. 34 (1991) 2063–2070.
[14] K. Jambunathan, S.L. Hartle, S. Ashforth-Frost, V.N. Fontama, Evaluating convective heat transfer coefficients using neural networks, Int. J. Heat Mass Transf. 39 (1996) 2329–2332.
[15] A. Alizadehdakhel, M. Rahimi, J. Sanjari, A.A. Alsairafi, CFD and artificial neural network modeling of two-phase flow pressure drop, Int. Commun. Heat Mass Transf. 36 (2009) 850–856.
[16] M.S. Shadloo, A. Rahmat, A. Karimipour, S. Wongwises, Estimation of pressure drop of two-phase flow in horizontal long pipes using artificial neural networks, J. Energy Resour. Technol. 142 (2020), https://doi.org/10.1115/1.4047593.
[17] J.J. Garcia, F. Garcia, J. Bermudez, L. Machado, Prediction of pressure drop during evaporation of R407C in horizontal tubes using artificial neural networks, Int. J. Refrig. 85 (2018) 292–302.

[18] G.A. Longo, S. Mancin, G. Righetti, C. Zilio, R. Ceccato, L. Salmaso, Machine learning approach for predicting refrigerant two-phase pressure drop inside Brazed Plate Heat Exchangers (BPHE), Int. J. Heat Mass Transf. 163 (2020), 120450.
[19] J.M. Barroso-Maldonado, J.A. Montanez-Barrera, J.M. Belman-Flores, S.M. Aceves, ANN-based correlation for frictional pressure drop of non-azeotropic mixtures during cryogenic forced boiling, Appl. Therm. Eng. 149 (2019) 492–501.
[20] B. Najafi, K. Ardam, A. Hanusovsky, F. Rinaldi, L.P.M. Colombo, Machine learning based models for pressure drop estimation of two-phase adiabatic air-water flow in micro-finned tubes: determination of the most promising dimensionless feature set, Chem. Eng. Res. Des. 167 (2021) 252–267.
[21] K. Ardam, B. Najafi, A. Lucchini, F. rinaldi, L.P.M. Colombo, Machine learning based pressure drop estimation of evaporating R134a flow in micro-fin tubes: Investigation of the optimal dimensionless feature set, Int. J. Refrig. 131 (2021) 20–32.
[22] A. Lopez-Belchi, F. Illan-Gomez, J.M. Cano-Izquierdo, J.R. Gracia-Cascales, GMDH ANN to optimise model development: Prediction of the pressure drop and the heat transfer coefficient during condensation within mini-channels, Appl. Therm. Eng. 144 (2018) 321–330.
[23] A. Khosravi, J.J.G. Pabon, R.N.N. Koury, L. Machado, Using machine learning algorithms to predict the pressure drop during evaporation of R407C, Appl. Therm. Eng. 133 (2018) 361–370.
[24] Y. Qiu, D. Garg, S.M. Kim, I. Mudawar, C.R. Kharangate, Machine learning algorithms to predict flow boiling pressure drop in mini/micro-channels based on universal consolidated data, Int. J. Heat Mass Transf. 178 (2021), 121607.
[25] F. Nie, S. Yan, H. Wang, C. Zhao, Y. Zhao, M. Gong, A universal correlation for predicting two-phase frictional pressure drop in horizontal tubes based on machine learning, Int. J. Multiph. Flow 160 (2023), 104377.
[26] D.E. Rumelhart, G.E. hinton, R.J. Williams, Learning internal representations by error propagation (No. Ics-8506), Calif Univ San Diego La Jolla Inst Cogn Sci (1986) 318-362, 10.1016/B978-1-4832-1446-7.50035-2.
[27] S.Z. Rouhani, E. Axelsson, Calculation of void volume fraction in the subcooled and quality boiling regions, Int. J. Heat Mass Transf. 13 (1970) 383–393.
[28] X. Wu, Y. Zhu, Y. Tang, New experimental data of CO2 flow boiling in mini tube with micro fins of zero helix angle, Int. J. Refrig. 59 (2015) 281–294.
[29] M. Wetzel, B. Dietrich, T. Wetzel, Influence of oil on heat transfer and pressure drop during flow boiling of CO2 at low temperatures, Exp. Therm. Fluid Sci. 59 (2014) 202–212.
[30] N. Pehlivanoglu, S. Kim, P.S. Hrnjak, Effect of oil on heat transfer and pressure drop of R744 in 6.1 mm horizontal smooth tube, Int. Refrig. Air Cond. Conf. (2010). Paper 1125, http://docs.lib.purdue.edu/iracc/1125.
[31] R. Mastrullo, A.W. Mauro, A. Rosato, G.P. Vanoli, Carbon dioxide heat transfer coefficients and pressure drops during flow boiling: assessment of predictive methods, Int. J. Refrig. 33 (2010) 1068–1085.
[32] J. Wu, T. Koettig, C. Franke, D. Helmer, T. Eisel, F. Haug, J. Bremer, Investigation of heat transfer and pressure drop of CO2 two-phase flow in a horizontal minichannel, Int. J. Heat Mass Transf. 54 (2011) 2154–2162.
[33] C.Y. Park, P.S. Hrnjak, CO2 and R410A flow boiling heat transfer, pressure drop, and flow pattern at low temperatures in a horizontal smooth tube, Int. J. Refrig. 30 (2007) 166–178.
[34] J.M. Cho, M.S. Kim, Experimental studies on the evaporative heat transfer and pressure drop of CO2 in smooth and micro-fin tubes of the diameters of 5 and 9.52 mm, Int. J. Refrig. 30 (2007) 986–994.
[35] J. Pettersen, Flow vaporization of CO2 in microchannel tubes, Exp. Therm. Fluid Sci. 28 (2004) 111–121.
[36] J. Pettersen, Flow vaporization of CO2 in microchannel tubes, Doctoral Thesis, NTNU 2002.
[37] S. Grauso, R. Mastrullo, A.W. Mauro, G.P. Vanoli, Two-phase adiabatic frictional pressure gradients for R410A and CO2 in a macro channel: Experiments and a simplified predictive method for annular flow from low to medium reduced pressure, Exp. Therm. Fluid Sci. 52 (2014) 79–87.
[38] T. Ono, L. Gao, T. Honda, Heat transfer and flow characteristics of flow boiling of CO2-oil mixtures in horizontal smooth and micro-fin tubes, Heat Transf. Asian Res. 39 (2010) 195–207.
[39] S. Kim, P. Hrnjak, Effect of oil on flow boiling heat transfer and flow patterns of CO2 in 11.2 mm horizontal smooth and enhanced tube, Int. Refrig. Air Cond. Conf. (2012). Paper 1331, http://docs.lib.purdue.edu/iracc/1331.
[40] M. Katsuta, K. Okuma, T. Hirade, N. Miyachi, The effect of the lubricating oil fraction rate on the CO2 evaporating thermal and hydraulic characteristics, Int. Refrig. Air Cond. Conf. (2008). Paper 910, http://docs.lib.purdue.edu/iracc/910.
[41] D. Del Col, M. Bortolato, S. Bortolin, Comprehensive experimental investigation of two-phase heat transfer and pressure drop with propane in a minichannel, Int. J. Refrig. 47 (2014) 66–84.
[42] G. Lillo, R. Mastrullo, A.W. Mauro, L. Viscito, Flow boiling heat transfer, dry-out vapor quality and pressure drop of propane (R290): Experiments and assessment of predictive methods, Int. J. Heat Mass Transf. 126 (2018) 1236–1252.
[43] R. Charnay, R. Revellin, J. Bonjour, Discussion on the validity of prediction tools for two-phase flow pressure drops from experimental data obtained at high saturation temperatures, Int. J. Refrig. 54 (2015) 98–125.
[44] D.F. Sempertegui-Tapia, G. Ribatski, Two-phase frictional pressure drop in horizontal micro-scale channels: experimental data analysis and prediction method development, Int. J. Refrig. 79 (2017) 143–163.
[45] M. Padilla, R. revellin, P. Haberschill, A. Bensafi, J. Bonjour, Flow regimes and two-phase pressure gradient in horizontal straight tubes: experimental results for HFO-1234yf, R-134a and R-410A, Exp. Therm. Fluid Sci. 35 (2011) 1113–1126.
[46] D. Del Col, A. bisetto, M. Bortolato, D. Torresin, L. Rossetto, Experiments and updated model for two-phase frictional pressure drop inside minichannels, Int. J. Heat Mass Transf. 67 (2013) 326–337.
[47] G.A. Longo, S. Mancin, G. Righetti, C. Zilio, Saturated vapour condensation of HFC404A inside a 4 mm ID horizontal smooth tube: comparison with the long-term low GWP substitutes HC290 (propane) and HC1270 (propylene), Int. J. Heat Mass Transf. 108 (2017) 2088–2099.
[48] G.A. Longo, S. Mancin, G. Righetti, C. Zilio, Saturated vapour condensation of R410A inside a 4 mm ID horizontal smooth tube: comparison with the low GWP substitute R32, Int. J. Heat Mass Transf. 125 (2018) 702–709.
[49] Q. Song, G. Chen, H. Guo, J. Shen, M. Gong, Two-phase flow condensation pressure drop of R14 in a horizontal tube: Experimental investigation and correlation development, Int. J. Heat Mass Transf. 139 (2019) 330–342.
[50] J.D. de Oliveira, J.B. Copetti, J.C. Passos, Experimental investigation on flow boiling pressure drop of R-290 and R-600a in a horizontal small tube, Int. J. Refrig. 84 (2017) 165–180.
[51] J.G. Pabon, A. Khosravi, R. Nunes, L. Machado, Experimental investigation of pressure drop during two-phase flow of R1234yf in smooth horizontal tubes with internal diameters of 3.2 mm to 8.0 mm, Int. J. Refrig. 104 (2019) 426–436.
[52] G. Lillo, R. Mastrullo, A.W. Mauro, L. Viscito, Flow boiling of R32 in a horizontal stainless steel tube with 6.00 mm ID. Experiments, assessment of correlations and comparison with refrigerant R410A, Int. J. Refrig. 97 (2019) 143–156.
[53] S. Grauso, R. Mastrullo, A.W. Mauro, J.R. Thome, G.P. Vanoli, Flow pattern map, heat transfer and pressure drops during evaporation of R-1234ze(E) and R134a in a horizontal, circular smooth tube: experiments and assessment of predictive methods, Int. J. Refrig. 36 (2013) 478–491.
[54] M. Ducoulombier, S. Colasson, J. Bonjour, P. Haberschill, Carbon dioxide flow boiling in a single microchannel - Part I: Pressure drops, Exp. Therm. Fluid Sci. 35 (2011) 581–596.
[55] H. Fazelnia, S. Azarhazin, B. Sajadi, M.A.A. Behabadi, S. Zakeralhoseini, M. V. Rafienejad, Two-phase R1234yf flow inside horizontal smooth circular tube: heat transfer, pressure drop, and flow pattern, Int. J. Multiph. Flow 140 (2021), 103668.
[56] J.M. quiben, J.R. Thome, Flow pattern based two-phase frictional pressure drop model for horizontal tubes. Part I: diabatic and adiabatic experimental study, Int. J. Heat Fluid Flow 28 (2007) 1049–1059.
[57] X.R. Zhuang, M.Q. Gong, X. Zou, G.F. Chen, J.F. Wu, Experimental investigation on flow condensation heat transfer and pressure drop of R170 in a horizontal tube, Int. J. Refrig. 66 (2016) 105–120.
[58] X.R. zhuang, G.F. Chen, X. Zou, Q.L. Song, M.Q. Gong, Experimental investigation on flow condensation of methane in a horizontal smooth tube, Int. J. Refrig. 78 (2017) 193–214.
[59] A. Cavallini, G. Censi, D. Del Col, L. Doretti, G.A. Longo, L. Rossetto, Experimental investigation on condensation heat transfer and pressure drop of new HFC refrigerants (R134a, R125, R32, R410A, R236ea) in a horizontal smooth tube, Int. J. Refrig. 24 (2001) 73–87.
[60] X. Chen, Y. Hou, S. Chen, X. Liu, X. Zhong, Characteristics of frictional pressure drop of two-phase nitrogen flow in horizontal smooth mini channels in diabatic/adiabatic conditions, Appl. Therm. Eng. 162 (2019), 114312.
[61] M. Zhang, R.L. Webb, Correlation of two-phase friction for refrigerants in small-diameter tubes, Exp. Therm. Fluid Sci. 25 (2001) 131–139.
[62] G.A. Longo, S. Mancin, G. Righetti, C. Zilio, Saturated vapour condensation of R134a inside a 4 mm ID horizontal smooth tube: comparison with the low GWP substitutes R152a, R1234yf and R1234ze(E), Int. J. Heat Mass Transf. 133 (2019) 461–473.
[63] C. Qi, X. Chen, W. Wang, J. Miao, H. Zhang, Experimental investigation on flow condensation heat transfer and pressure drop of nitrogen in horizontal tubes, Int. J. Heat Mass Transf. 132 (2019) 958–996.
[64] R. Revellin, J.R. Thome, Adiabatic two-phase frictional pressure drops in microchannels, Exp. Therm. Fluid Sci. 31 (2007) 673–685.
[65] A. Arcasi, R. Mastrullo, A.W. Mauro, L. Viscito, Adiabatic frictional pressure gradient during flow boiling of pure refrigerant R1233zd and non-azeotropic mixtures R448A, R452A and R455A, JoP Sci. Conf. Ser. 2177 (2022), 012045, https://doi.org/10.1088/1742-6596/2177/1/012045.
[66] R.J. da Silva Lima, J.M. Quiben, C. Kuhn, T. Boyman, J.R. Thome, Ammonia two-phase flow in a horizontal smooth tube: flow pattern observations, diabatic and adiabatic frictional pressure drops and assessment of prediction methods, Int. J. Heat Mass Transf. 52 (2009) 2273–2288.
[67] J. Qiu, H. Zhang, Experimental investigation on two-phase frictional pressure drop of R600a and R600a/3GS oil mixture in a smooth horizontal tube, Int. J. Refrig. 117 (2020) 307–315.
[68] M.K. Bashar, K. Nakamura, K. Kariya, A. Miyara, Development of a correlation for pressure drop of two-phase flow inside horizontal small diameter smooth and microfin tubes, Int. J. Refrig. 119 (2020) 80–91.
[69] C. Aprea, A. Greco, A. Rosato, Comparison of R407C and R417A heat transfer coefficients and pressure drops during flow boiling in a horizontal smooth tube, Energy Convers. Manage. 49 (2008) 1629–1636.
[70] Y. Xu, Z. Yan, L. Li, Flow boiling heat transfer, pressure drop and flow patterns of the environmentally friendly refrigerant R1234yf for cooling avionics, Appl. Therm. Eng. 209 (2022), 118301.
[71] C.Y. Yang, H. Nalbandian, F.C. Lin, Flow boiling heat transfer and pressure drop of refrigerants HFO-1234yf and HFC-134a in small circular tube, Int. J. Heat Mass Transf. 121 (2018) 726–735.
[72] M.I. Zakaria, M.A. Akhavan-Behabadi, B. Sajadi, M.T. Moghadam, An empirical investigation on flow pattern, heat transfer, and pressure drop during flow boiling of R1234yf in an inclined plain tube, Int. J. Therm. Sci. 170 (2021), 107100.

[73] X. Chen, S. Chen, J. Chen, J. Li, X. Liu, L. Chen, Y. Hou, Two-phase flow boiling frictional pressure drop of liquid nitrogen in horizontal circular mini-tubes: Experimental investigation and comparison with correlations, Cryogenics 83 (2017) 85–94.
[74] M.H. Maqbool, B. Palm, R. Khodabandeh, Flow boiling of ammonia in vertical small diameter tubes: two-phase frictional pressure drop results and assessment of prediction methods, Int. J. Therm. Sci. 54 (2012) 1–12.
[75] A. Cicchitti, C. Lombardi, M. Silvestri, G. Soldaini, R. Zavattarelli, Two-phase cooling experiments: pressure drop, heat transfer and burnout measurements, Energia Nucl. 7 (1960) 407–425.
[76] A.W. Mauro, L. Viscito, R. Revellin, Void fraction and pressure gradient model for an adiabatic symmetric annular developed flow with entrainment, Int. J. Multiph. Flow 153 (2022), 104126.
[77] L. Cheng, G. Ribatski, L. Wojtan, J.R. Thome, New flow boiling heat transfer model and flow pattern map for carbon dioxide evaporating inside horizontal tubes, Int. J. Heat Mass Transf. 49 (2006) 4082–4094.
[78] L. Wojtan, T. Ursenbacher, J.R. Thome, Investigation of flow boiling in horizontal tubes: part I - A new diabatic two-phase flow pattern map, Int. J. Heat Mass Transf. 48 (2005) 2955–2969.